10032–10041 *Nucleic Acids Research, 2017, Vol. 45, No. 17* *Published online 20 July 2017*
doi: 10.1093/nar/gkx628

Parallel triplex structure formed between stretched single-stranded DNA and homologous duplex DNA

Jin Chen[1], Qingnan Tang[2], Shiwen Guo[1], Chen Lu[1,3], Shimin Le[1,2] and Jie Yan[1,2,3,*]

[1]Mechanobiology Institute, National University of Singapore, 117411, Singapore, [2]Department of Physics, National University of Singapore, 117542, Singapore and [3]Centre for Bioimaging Sciences, National University of Singapore, 117546, Singapore

Received January 23, 2017; Revised July 08, 2017; Editorial Decision July 10, 2017; Accepted July 11, 2017

ABSTRACT

The interaction between the single-stranded DNA and the homologous duplex DNA is essential for DNA homologous repair. Here, we report that parallel triplex structure can form spontaneously between a mechanically extended ssDNA and a homologous dsDNA in protein-free condition. The triplex has a contour length close to that of a B-form DNA duplex and remains stable after force is released. The binding energy between the ssDNA and the homologous dsDNA in the triplex is estimated to be comparable to the basepairing energy in a B-form dsDNA. As ssDNA is in a similar extended conformation within recombinase-coated nucleoprotein filaments, we propose that the parallel triplex may form and serve as an intermediate during recombinase-catalyzed homologous joint formation.

INTRODUCTION

Homologous recombination (HR), which is catalyzed by recombinases such as RecA or Rad51, is necessary for various crucial processes that take place on chromosomes, such as DNA damage repair and meiosis (1). A critical step of HR in these processes involves homologous search, during which the single-stranded DNA (ssDNA) in the recombinase-coated nucleoprotein filament reads the sequence information in the associating double-stranded DNA (dsDNA) to determine the homology, which takes place through the alignment and pairing between ssDNA bases inside the nucleoprotein filament and the basepairs in the homologous duplex DNA. After homology search, the ssDNA inside the recombinase nucleoprotein filament exchanges with the homologous strand inside duplex DNA and forms a heteroduplex DNA.

The ssDNA inside the RecA nucleoprotein filament adopted an extended overall conformation, which is about 1.5 times of the contour length of the B-form DNA duplex of the same number of basepairs (2–7). The ssDNA in the nucleoprotein filament is base-stacked and right-handed consisting of repeating units of 3-nt (triplet) per RecA protomer with a large axial rise (7.8 Å) between each triplet (5). Recent electron microscopy study also suggested that ssDNA in the Rad51 filament assumes a similar conformation to that in the RecA filament (8). These results suggest that the duplex DNA needs to be extended non-uniformly in order to align with the ssDNA inside the recombinase nucleoprotein filament during homologous joint formation (9–11).

The exact mechanism underlying homology recognition has not been fully understood. In the simplest picture, homology could be recognized through Watson–Crick basepairing between the ssDNA strand in the RecA/Rad51 nucleoprotein filament and the complementary strand in the substrate dsDNA. This mechanism implies transient local disruption of the Watson–Crick basepairs in the dsDNA (12,13). Recent single-molecule imaging studies showed that homologous recognition of the RecA/Rad51 filament occurred in precise 3-nt steps, and robust homologous selection required at least 8 nt of local homology (14,15).

It has been shown that the homologous joint molecule formed after RecA-mediated base pair switch is a triple-stranded structure in which the ssDNA forms a heteroduplex with the complementary strand in the dsDNA through Watson–crick base pairing and the outgoing strand binds to the major groove of the heteroduplex (9). In this joint molecule, the outgoing strand and the heteroduplex DNA are all held in an extended structure (16). It is known that a large force of more than 60 pN is needed to elongate a dsDNA duplex beyond its B-form contour length (17,18), and an energy cost of $\sim 2\, k_B T$ per base pair step can be estimated to elongate dsDNA by 1.5 folds (19,20). Therefore, a large amount of energy is needed to keep the heteroduplex in the extended conformation in the RecA-associated joint molecule, which might be provided by RecA–DNA interaction (21–24), heteroduplex and outgoing strand interaction, or both.

Here, we report a spontaneous formation of a parallel triplex between a mechanically extended ssDNA and dsDNA in solution in protein-free condition. The interac-

*To whom correspondence should be addressed. Tel: +65 65162620; Fax: +65 67776126; Email: phyyj@nus.edu.sg

tion between the extended ssDNA and dsDNA in solution is monitored by an in-house built magnetic tweezers setup (25). The homology requirement of the triplex formation implies that the ssDNA strand must be in an orientation parallel to the identical strand inside the duplex DNA, which differs from the canonical triplex that forms on homopurine-homopyrimidin stretches with the third strand anti-parallel to the chemically homologous strand inside the duplex DNA (26). The triplex has a contour length close to a B-form DNA duplex, which is strongly promoted by mechanical forces of 8–42 pN applied to the third strand. The triplex can form against large tensile forces, associated with large extension decreases, indicating a strong interaction between the ssDNA and the homologous dsDNA.

MATERIALS AND METHODS

Magnetic tweezers experiments

An in-house built magnetic tweezers apparatus was used in this study with a spatial resolution of 2 nm and a sampling rate of 200 Hz (25). Force calibration has an intrinsic relative error around 10%, which is caused by the uncertainty of the radius of M280 Dynabeads (Thermo Scientific) used in the experiments. Details of force calibration and force error can be found in our previous publication (25). A disturbance-free buffer exchange system was used to observe real-time dynamics of DNA extension change (27). Experimental data included in the main text were carried out at 23°C under the following buffer conditions unless otherwise indicated: 150 mM KCl, 30 mM Tris (pH = 7.4). Some experiments were conducted under three other solution conditions (data are included in Supplementary Data): 150 mM KCl, 5 mM $MgCl_2$, 30 mM Tris (pH = 7.4); 50 mM KCl, 30 mM Tris (pH = 7.4); 50 mM NaCl, 10 mM $MgCl_2$, 30 mM Tris (pH = 7.4).

DNA and protein materials

572-bp dsDNA with the 3′ and 5′ ends of one strand labeled with Biotin and a Thiol group was generated using the DreamTaq (Thermo Scientific) catalyzed polymerase chain reaction (PCR) as illustrated in previous studies (7,28). 572-nt of ssDNA was generated by a force-induced strand-peeling transition of the 572-bp dsDNA in 25 mM Tris (pH = 7.4). Blunt-ended homologous, non-homologous 572-, 654- and 150-bp dsDNA were generated by PCR catalyzed by Q5 polymerase (NEB) using lambda phage DNA as a template. These dsDNA molecules were further purified in two different ways: gel extraction using the PureLink kit (Invitrogen) and Exonuclease I treatment. 5′-Biotin-labeled 593-bp dsDNA and 5′-thiol-labeled 481-bp dsDNA handles were prepared by DreamTaq (Thermo Scientific) catalyzed PCR using lambda phage DNA as a template. The PCR product was further purified using a PCR purification kit and digested with the BstXI restriction enzyme (NEB). The 200-nt ssDNA was annealed with two flank oligos and then ligated with the two handles (481- and 593-bp) using DNA ligation Mix (TARAYA) and purified by gel extraction with the PureLink kit as illustrated in previous studies (29). All oligonucleotides in this study were ordered from Integrated DNA Technologies (IDT). Human Replication protein A (RPA) was provided by our collaborator (Prof. Walter Chazin, Vanderbilt University), which was purified as described previously (30). dsDNase (ThermoFisher) is a commercially available dsDNA-specific cutting enzyme and the dsDNase cutting assay is conducted using 50 times dilution from the stock concentration in 1× dsDNase solution.

Data processing

All experimental data were processed with Origin 9.0. Time trace extension dynamics were smoothed using a built-in fast fourier transformation (FFT) filter with a time interval of 0.1 s. The initial extension from multiple traces was shifted to 285 nm for the convenience of step-size comparison. The shift in the initial extension does not affect step-size determination.

RESULT

Single-molecule experiments reveal a stable parallel DNA triplex

To probe potential homologous interactions between ssDNA and dsDNA, we stretched a single ssDNA (572-nt) using a magnetic tweezers setup (25) (Figure 1A). We introduced homologous dsDNA molecules of the same number of base pairs into the solution, and detected potential interactions between the ssDNA and dsDNA based on the resulting changes in ssDNA extension.

We observed time traces of the ssDNA extension upon the introduction of homologous dsDNA when a force of 21.0 ± 2.1 pN was applied to the ssDNA (Figure 1B). Large stepwise decreases in extension were observed for 368.6 ± 25.4 s (mean ± standard error) after the 50 nM dsDNA solution was introduced (Supplementary Figure S1A). Similar results were obtained in more than 100 independent experiments over a wide range of forces from 8 to 42 pN under buffer conditions ranging from 50 to 150 mM KCl and 30 mM Tris (pH = 7.4) with or without 5 mM $MgCl_2$. In all of these experiments, interactions between ssDNA and homologous dsDNA led to unidirectional extension decreases to different extents within our experimental time scale up to 2000 s (Supplementary Figure S1B). The 0.1 s zoom-in of the extension decrease steps did not show any intermediate steps, indicating triplex formation upon dsDNA binding with a very fast progression rate that is difficult to be resolved at the sampling rate of our instrument (Supplementary Figure S2).

The possibility of contamination of complementary ssDNA in solution was ruled out by several means. The introduced dsDNA was either purified via agarose gel extraction or treated with ssDNA nuclease Exonuclease I. The same phenomenon was observed for purified dsDNA. Additionally, dsDNA of the same length with non-homologous sequences was also tested; however, ssDNA extension drop was not observed (Supplementary Figure S3). Therefore, we conclude that there is direct interaction between the ssDNA and the homologous dsDNA, which results in the formation of a triplex structure comprised of three DNA strands.

In the above experiments, the ssDNA and dsDNA have the same number of base pairs/nucleotides. To see whether this interaction could take place on a homologous region

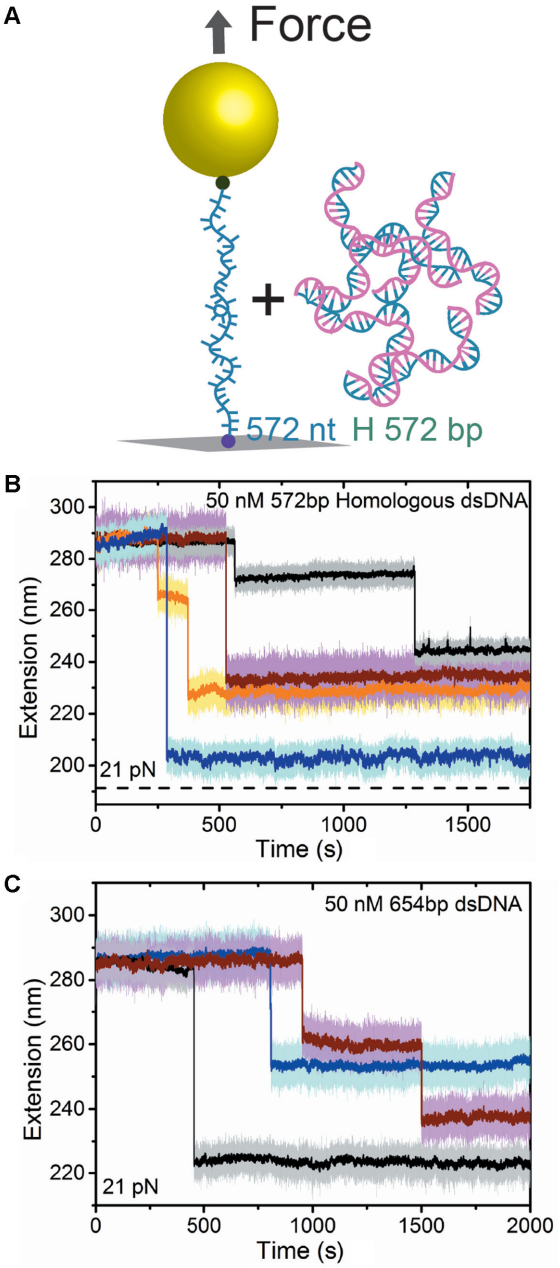

Figure 1. Dynamics of the parallel DNA triplex formation. (**A**) Schematic of the magnetic tweezers manipulation experiments in which homologous 572-bp dsDNA was introduced to a 572-nt ssDNA tethered between a coverslip and a paramagnetic bead. (**B** and **C**) Representative time traces of the changes in extension of the ssDNA in the presence of 50 nM 572-bp homologous dsDNA (B) or in the presence of 50 nM 654-bp dsDNA with 561-bp homologous sequence in the middle (C) under a constant force of 21 pN. The abrupt decreases in extension in (B) and (C) were due to interactions between the ssDNA and the homologous dsDNA. The dashed black line in (B) indicates the extension of 572-bp dsDNA under the same force.

inside the dsDNA region, we sandwiched a 561-bp homologous sequence between two non-homologous handles (45- and 48-bp, respectively). Extension drop of the tethered ssDNA was observed when the experiments were repeated using this dsDNA construct (Figure 1C). Therefore, this interaction can take place in a homologous region in the middle of the dsDNA. Hereafter, we refer to this complex as parallel triplex since it is formed between homologous duplex DNA and ssDNA with orientation parallel to the identical strand inside the duplex DNA.

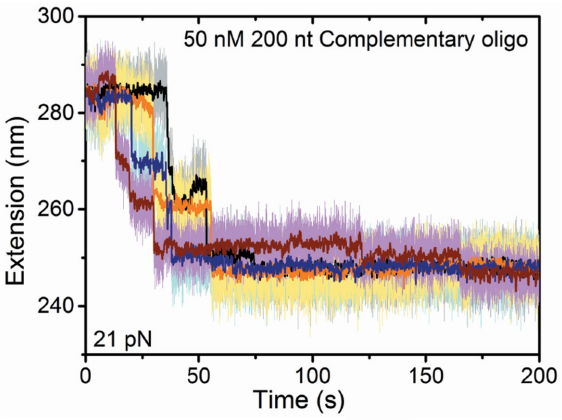

Figure 2. Dynamics of DNA duplex formation. Four representative extension time traces of a 572-nt ssDNA after introducing 50 nM of complementary 200-nt ssDNA at 21 pN. Colored centerlines are smoothed data using a fast fourier transition (FFT) filter with 0.1-s time interval.

Parallel triplex formation has different dynamics than duplex annealing

To compare the similarities and differences between parallel triplex formation and duplex formation that involves two complementary ssDNA strands, we did ssDNA hybridization experiment by introducing 50 nM of 200-nt complementary ssDNA to the tethered ssDNA. We observed duplex annealing interaction at 30.8 ± 2.2 s after introducing the ssDNA solution, indicated by progressive reduction of the extension of the ssDNA tether against 21 pN (Figure 2). After the annealing interaction started, it took 98.0 ± 13.3 s to reach a final steady state with a total decrease in extension of 34.7 ± 3.3 nm.

The duplex annealing dynamics in Figure 2 shows that annealing caused stepwise shortening in extension. However, there were several notable differences between annealing and parallel triplex formation. First, the annealing reaction started within around 30 s after introducing the complementary strands of the same concentration, which is much faster than that observed for triplex formation (around 400 s at 21 pN after introducing the homologous dsDNA at the same concentration) (Supplementary Figure S4). Furthermore, duplex annealing reaches a well-defined steady state within 200 s, which is around 35 nm shorter than the extension before annealing occurred.

This ∼35 nm extension decrease is consistent with the extension difference expected between a 200-nt ssDNA and a 200-bp dsDNA at 21 ± 2.1 pN (Supplementary Figure S5), which starkly contrasts to what happened in the formation of the parallel triplex, wherein the final extensions varied significantly even at a much longer time scale of 2000 s. The duplex annealing process consists of three to four steps with step sizes smaller than those observed for triplex formation

(Supplementary Figure S6). Together, these differences indicate that the formation of a parallel triplex has markedly different dynamics than duplex formation.

Parallel triplex structures and unoccupied ssDNA co-exist in the reaction product

As shown in Figure 1B, over the experimental time scale up to 2000 s, the final extensions after the formation of a parallel triplex differ significantly in different experiments, which suggests that the reaction might not reach a steady state within this time scale. The shortest final extension is very close to dsDNA, indicating a complete parallel triplex may have a similar contour length to dsDNA with the corresponding number of base pairs, which is consistent with the 0.32 nm contour length reported in previous X-ray studies on the $(G^*GC)_2$ parallel triplex (31). If this is the case, one may expect that the reaction products might be a mixture of the parallel triplex and unoccupied ssDNA.

If we substitute the force responses of a parallel triplex as the duplex DNA with a helical rise of 0.34 nm, the fraction of ssDNA occupied in a region of triplex can be estimated by $\alpha = \Delta/(x_{572\text{-}nt\ ssDNA}(F) - x_{572\text{-}bp\ dsDNA}(F))$, where $x_{572\text{-}nt\ ssDNA}(F) - x_{572\text{-}bp\ dsDNA}(F)$ is the difference in extension between a 572-nt ssDNA and a 572-bp dsDNA at a force of F, and Δ is the actual magnitude of the decrease in extension after parallel triplex formation. Based on this, the estimated fraction of ssDNA occupied in the parallel triplex region of the 572-nt long ssDNA spans a wide range of 15–98% based on more than 100 different experiments (Supplementary Figure S7). The fraction estimated based on the parallel triplex structure formed by $(G^*GC)_2$ with a helical rise of 0.32 nm (31) only differs by <10%.

The above estimation implies that a significant fraction of the ssDNA is outside the parallel triplex region and that this fraction of ssDNA may be accessible to ssDNA binding proteins. This was tested by introducing 100 nM full-length human RPA after a parallel triplex was formed at ~21 pN (Figure 3A). In this example, the parallel triplex formation resulted in a stepwise decrease in extension by ~59 nm, corresponding to α ~61.5% of the triplex region and ~38.5% of the ssDNA fraction.

As our previous study showed that the binding of RPA to ssDNA results in a significant increase in the extension of the ssDNA at low forces (<15 pN) (32), we reduced the force to 12 pN and introduced 100 nM RPA. After the introduction of full-length RPA, we observed an increase in the extension of ~11 nm, indicating that there was indeed a fraction of ssDNA exposed and available for RPA binding. At 100 nM concentration, the full-length RPA binding to ssDNA at 12 pN results in an increase in the extension of ~0.06 nm per nt (Supplementary Figure S8); hence, there were around 190 nt (~33.2%) of ssDNA exposed and available for RPA binding in this particular experiment. This leads to an estimation of the ~66.7% of ssDNA occupied in the parallel triplex region, which is almost consistent with the value of α ~61.5% estimated based on the equation $\alpha = \Delta/(x_{572\text{-}nt\ ssDNA}(F) - x_{572\text{-}bp\ dsDNA}(F))$.

In addition, we performed force-decrease scans followed by force-increase scans for the original dsDNA, tethered ssDNA, after triplex formation and after RPA introduction (Figure 3B). The possibility of RPA invading the parallel triplex region was ruled out by comparing the force-extension curve of the parallel triplex (orange) and RPA-bound the parallel triplex (blue), which shows similar extension at high forces, indicating that the parallel triplex region remains the same before and after RPA introduction. The consistency of the fraction of ssDNA bound in the parallel triplex estimated by the two methods was observed in multiple experiments (Supplementary Table S1). Together, these experiments strongly suggest that a stable parallel triplex region and unoccupied ssDNA co-exist in the reaction product within our experimental time scale.

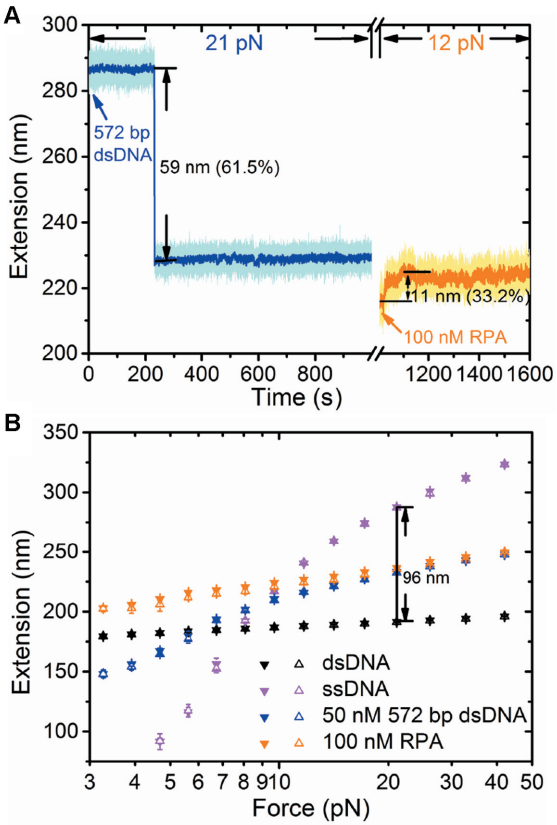

Figure 3. Co-existence of the parallel triplex and ssDNA. (**A**) A representative extension time trace of an ssDNA after introducing 50 nM homologous 572-bp dsDNA at 21 pN (blue) and after introducing 100 nM RPA at 12 pN (orange). The break in middle denotes the point at which free dsDNA was washed away and the force was changed from 21 to 12 pN. Colored centerlines are smoothed data using an FFT filter with 0.1 s time interval. (**B**) The force-extension curves of the 572-nt dsDNA (black), naked 572-nt ssDNA (violet), after a fraction of the ssDNA was occupied in the triplex region (blue) and after introduction of 100 nM RPA (orange).

The parallel triplex can be cleaved by dsDNase

The observed parallel triplex might involve two possible structures: (i) the mechanically stretched ssDNA forms additional hydrogen bonds with the introduced homologous duplex DNA and (ii) the mechanically stretched ssDNA forms a heteroduplex with the complementary strand in the incoming homologous duplex DNA through Watson–Crick hydrogen bonds, with displaced strand forming addi-

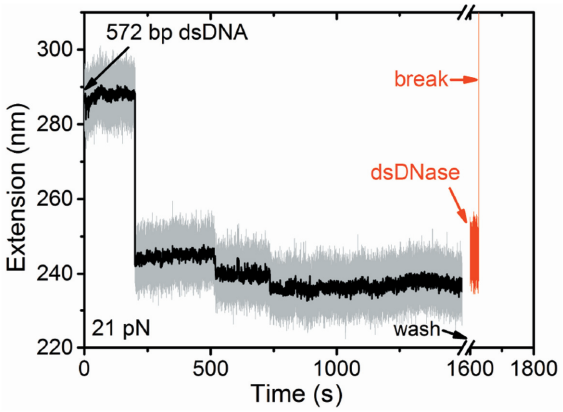

Figure 4. Cutting of a parallel triplex by dsDNase. After a parallel triplex was formed at 21 pN (black) on a 572-nt ssDNA, free dsDNA was removed by exchanging the solution to 1× dsDNase buffer solution. Then, dsDNase was introduced into the reaction chamber (red), which leads to the break of tether. The black centerline indicates smoothed data using an FFT filter with 0.1-s time interval.

tional hydrogen bonds with the heteroduplex DNA. Since the stretched ssDNA and the chemically identical strand in the dsDNA are indistinguishable in the parallel triplex, both forms may exist in different regions.

In order to obtain further insights into the structure of the parallel triplex, we applied dsDNA-specific cutting enzyme (dsDNase) treatment to the pre-formed parallel triplex. The dsDNase is a dsDNA-specific cutting endonuclease that cleaves phosphodiester bonds in DNA to yield oligonucleotides with 5′-phosphate and 3′-hydroxyl termini. In such experiments, the mechanically stretched ssDNA should remain intact in the case of the first proposed structure, while it might be cleaved in the second proposed structure. We repeated the parallel triplex formation experiment on a 572-nt ssDNA at 21.0 ± 2.1 pN and introduced dsDNase after parallel triplex formation (Figure 4). The break of tethered DNA was observed around 30 s after addition of dsDNase (50 times dilution from the stock concentration in 1× dsDNase buffer solution). To test the specificity of dsDNase on the duplex DNA, we applied dsDNase treatment on tethered pure ssDNA and observed that the ssDNA remains tethered in more than 500 s (Supplementary Figure S9). This result strongly suggests that the base pair switch takes place in the experiments.

Formation of the parallel triplex is promoted by the stretching of the ssDNA

The parallel triplex described in previous sections was formed under a condition where the ssDNA was stretched by forces ranging from 8 to 42 pN. To understand whether force played a role in the observed triplex formation, we repeated the experiments at a lower force of ∼0.7 pN. At this lower force, the ssDNA assumes a compact conformation; as a result, there is the risk that the bead may be pulled too close to the surface of the coverslip. Therefore, we used a gapped DNA in which a 164-nt ssDNA was spanned between two long dsDNA handles (606- and 485-bp) for this low force experiments. At ∼0.7 pN, the compact ssDNA

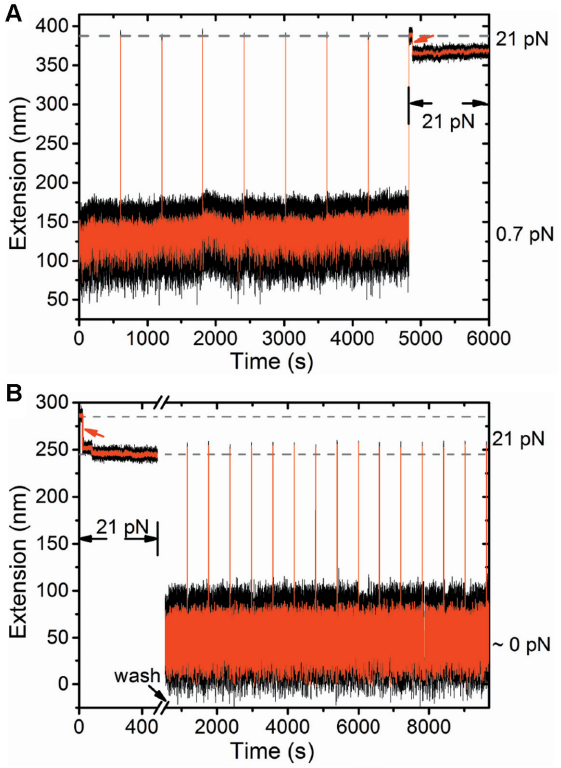

Figure 5. Force promotes parallel DNA triplex formation. (**A**) Extension time trace of a gapped 164-nt ssDNA upon introduction of homologous 150-bp dsDNA at 0.7 pN (50 nM). The force was shifted to 21 pN for 4 s after every 600 s, and the extension at the 21 pN was the same as the naked gapped DNA. After eight cycles, the force was clamped back at 21 pN. Within 50 s, a stepwise decrease in extension (arrow) indicated parallel triplex formation. (**B**) Extension time traces of a 572-nt ssDNA after introduction of homologous 572-bp dsDNA (50 nM) at 21 pN. A stepwise decrease in extension (arrow) indicates parallel triplex formation. After removal of free homologous dsDNA in the solution (break), the tether was held at near 0 pN and the force is shifted to 21 pN for 5 s after every 600 s, during which the extension at 21 pN remained at the same level after the parallel triplex formed. Dashed lines (gray) indicate the extension of tether before or after the formation of parallel triplexes at 21 pN. Red centerlines indicate smoothed data using an FFT filter with 0.1-s time interval.

had much shorter extension than a dsDNA of the same number of base pairs. Therefore, if a parallel triplex formed at this force, there should be an increase in extension. In addition, transient jumps to a greater force could also check the formation of the parallel triplex because there should be a decrease in extension at greater forces if a parallel triplex forms.

Using this new construct, within our experimental time scale up to 80 min after introducing 50 nM homologous 150-bp dsDNA, we did not observe extension increase at ∼0.7 pN or extension decrease after transient jump to ∼21 pN, indicating that the parallel triplex did not form at ∼0.7 pN over a long time scale of ∼4860 s (Figure 5A). In contrast, we observed parallel triplex formation on the same DNA construct within 50 s after the force was jumped to ∼21 pN at ∼4860 s and clamped at this force (Figure 5A). Based on these experiments, we conclude that the forces applied to the ssDNA play a critical role in promoting the formation of the parallel triplex described in previous sections.

It is also interesting to know whether mechanical stretching of the ssDNA is also needed to maintain a stable parallel triplex. To test the stability of the parallel triplex at lower forces, we repeated the parallel triplex formation experiment on a 572-nt ssDNA at 21.0 ± 2.1 pN and then reduced the force to near 0 pN. By holding the tether for 600 s and then shifting back to 21.0 ± 2.1 pN for 5 s, we found that the extension remained the same as that observed several hours after the formation of the parallel triplex, indicating that a preformed parallel triplex could remain stable for a long time after the force is released (Figure 5B).

Parallel triplex undergoes an 'overstretching' transition at ∼63 pN

To probe the force at which the parallel triplex would be destabilized, we performed force-increase scans followed by force-decrease scans using a force loading rate of 2 pN/s after parallel triplex formation. In the representative example shown in Figure 6A, at a force ∼63 pN, there was a significant increase in extension, which suggests that an 'overstretching' transition occurred. When the force was increased until the onset of the transition, the parallel triplex was partially overstretched and could be reversed by applying progressive decreases in the force applied (light blue and dark blue). In contrast, when the force was increased until the completion of the transition, the dsDNA dissociated and the tether became ssDNA again (black and gray). Such an overstretching transition of the parallel triplex was always observed for similar forces (∼63 pN) in all experiments.

The difference in the extension (δ) before and after the transition is proportional to the fraction (α) of ssDNA adsorbed into the parallel triplex. The results shown in the 'Parallel triplex structures and unoccupied ssDNA co-exist in the reaction product' section suggest that the parallel triplex has a similar contour length as dsDNA with the corresponding number of base pairs and a helical rise of h ∼0.34 nm between two adjacent triple bases. Using this approximation, we estimated the level of elongation during the overstretching transition of the parallel triplex using $\delta/\alpha Nh$ of ∼0.7, where δ is the change in extension after the overstretching transition, α is the fraction of ssDNA in the parallel triplex and $N = 572$ is the number of base pairs in the stretched ssDNA (Supplementary Figure S10). The level of elongation estimated using a helical rise of 0.32 nm (31) only differs by <10%. Therefore, our result indicates that overstretching led to ∼1.7 folds elongation of the parallel triplex.

The observed overstretching transition of the parallel triplex is very similar to the overstretching transition of dsDNA (Figure 6B), which occurs at similar forces and elongates to a similar extent (17,18). The overstretching transition of dsDNA mainly occurs via two competitive pathways: (i) a 'strand-peeling' pathway during which one strand is peeled away from the other, leaving one strand under force after the transition, and (ii) a 'B-to-S' transition pathway that leads to an elongated duplex structure without breaking the base pairs (19,20,33–36). The two pathways compete with each other according to various experimental conditions that affect DNA base pair stability (19,20,35,36).

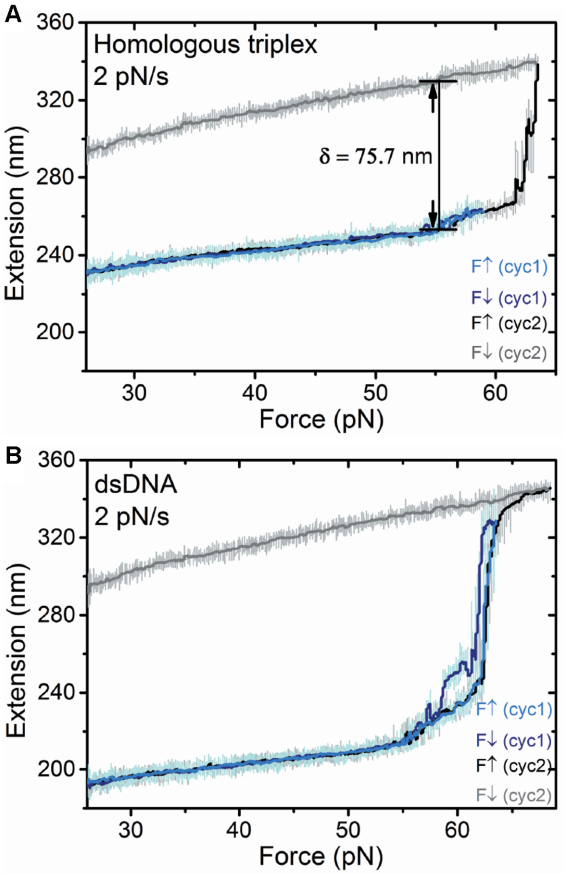

Figure 6. Parallel triplex undergoes an 'overstretching' transition. (**A**) Force-extension curves recorded in force loading cycles for a parallel triplex formed between a 572-bp dsDNA and a 572-nt ssDNA. The first cycle (cycle 1) includes a force-increase stage (light blue) where the force was increased by 2 pN/s till the onset of the overstretching transition, followed by a force-decrease stage (dark blue) with a loading rate of −2 pN/s. In the second cycle (cycle 2), during the force-increase stage (black), the force was increased till the completion of the overstretching transition. The subsequent force-decrease curve (dark gray) is the same as that of naked ssDNA, indicating the displacement of the dsDNA from the triplex. (**B**) Extension variation in the same force loading cycles performed for a 572-bp dsDNA shows a similarity between the triplex overstretching transition and the strand-peeling transition of the duplex. In panels (A) and (B), centerlines indicate smoothed data using an FFT filter with 0.1 s time interval.

In the case of overstretching of the parallel triplex, two possibilities exist regarding the state of the incoming dsDNA after the transition: (i) the dsDNA simply dissociated into solution and (ii) the two strands in the dsDNA also separated into two strands after dissociation. Comparing to the first scenario, the second scenario needs an additional energy to further disrupt the base pairs within duplex DNA. Therefore, between the two possibilities, the first one is much more energetically favorable than the second in spite of the fact that the exact overstretching transition pathway is still not clear. Since a complete transition resulted in displacement of the bound dsDNA, it resembles the well-known force-dependent strand-peeling transition of dsDNA. The similarities between the triplex overstretching transition and the stand-peeling transition of the B-form dsDNA suggest that ssDNA–dsDNA interaction energy is

likely comparable to the base pairing energy in the B-form dsDNA.

DISCUSSION

In this paper, we report a spontaneous formation of a highly stable parallel DNA triplex. The parallel triplex is formed between a mechanically extended ssDNA and the homologous dsDNA, with the ssDNA parallel to the identical strand inside the duplex DNA. The parallel triplex differs from the extensively studied anti-parallel DNA triplex formed on homopurine-homopyrimidin stretches through Hoogsteen or reversed Hoogsteen hydrogen bonds, in which the third strand is anti-parallel to the chemically homologous strand inside the dsDNA (26). We also observed an interesting overstretching transition of the parallel triplex at forces around 63 pN, which resulted in an increase in the extension and dissociation of the dsDNA after the transition. Both the transition force and the extent of DNA elongation are similar to the strand-peeling transition observed for the B-form dsDNA (37), which suggests that the interaction energy of the ssDNA and the homologous dsDNA is likely at a level similar to that of base pairing energy in a B-form dsDNA.

Within the typical experimental timescale up to 2000 s in our experiments, the final extensions of the tethered ssDNA after binding of a homologous dsDNA are highly varied. This is in stark contrast to annealing of 200-nt complementary ssDNA to the stretched ssDNA that always proceeds till full completion within 200 s. The incomplete parallel triplex formation compared to complete duplex annealing when the ssDNA was held at similar forces indicates that annealing between two complementary ssDNA is a robust process, while the formation of the parallel triplex between ssDNA and homologous dsDNA is sensitive to perturbations. This difference is likely related to different natures of these two processes. Although the cause of the incomplete triplex formation is unclear, we speculate that it might be related to local defects produced during triplex formation, which may cause pauses on its progression. For example, assuming the triplex formation involves a moving fork between ssDNA and dsDNA, there is a possibility that a micro-triplex formed at shifted position downstream to the fork might cause a global sequence misalignment that pauses the progression of triplex formation (Supplementary Figure S11).

The nature of the observed parallel triplex formation is unclear. One possibility is that the ssDNA binds the dsDNA in the major groove to form additional hydrogen bonds with the dsDNA. It is also possible that the ssDNA hybridizes with the complementary ssDNA strand in the dsDNA to form a heteroduplex, with the displaced strand binding the major groove of the heteroduplex. The latter structure was previously implied in the joint molecule catalyzed by RecA, which is a base pair-switched DNA triplex (9). It is noteworthy that the parallel triplex observed in our experiments was formed in the absence of any recombinase in our experiment. Since the ssDNA and the chemically identical strand in the dsDNA are indistinguishable in the triplex, both structures could form. In addition, the two forms of parallel triplex may co-exist in a dynamics manner considering the short base pair lifetime of dsDNA of around 10 ms (38). The fact that the triplex could be cleaved by dsDNase suggests that a base-pair switch took place, at least partly, in the observed triplex. During triplex formation, the additional hydrogen bonds formed between the ssDNA (either the original ssDNA or the displaced strand) with the duplex (either the original dsDNA or the heteroduplex) may compensate the energy for a large extension drop against the tensile force during triplex formation.

Compared to the rate of association of a complementary ssDNA strand to the stretched ssDNA ($\sim 3 \times 10^{-2}$ s^{-1} in 50 nM 200-nt ssDNA concentration), the homologous dsDNA has a much slower binding rate to the stretched ssDNA over a force range of 8–42 pN ($\sim 3 \times 10^{-3}$ s^{-1} in 50 nM 572-bp dsDNA concentration, Supplementary Figure S4). At near zero force, we never observed triplex formation over a very long experimental time scale (up to 5000 s). After binding, the formation of the parallel triplex is marked by an abrupt extension shortening of ssDNA. In the majority of such triplex formation events, no intermediate steps were detected after zoom-in to 0.1 s time intervals (Supplementary Figure S2). All these features indicate that the triplex formation is a highly cooperative process, which requires overcoming a high nucleation energy barrier for initial binding in a force-dependent manner. Formation of a nucleating triplex likely involves a sufficient number of nucleotides of the ssDNA in certain conformations. The force applied to the ssDNA may assist in providing such ssDNA conformation that is required for the formation of the nucleation site. It supports a view proposed in previous studies that homologous joint formation catalyzed by RecA/Rad51-recombinases depends on an intrinsic property or dynamics of DNA, where the RecA/Rad51-recombinases play a role to create a micro-environment that facilitates direct interaction between the DNA molecules (9,39). A similar mechanism may also apply to homologous joint formation mediated by eukaryotic Rad52, mitochondrial ribosomal Mhr1 and the β protein from *Escherichia coli* phage λ, which catalyze the base pair switch reactions in an adenosine triphosphate (ATP)-independent manner (40–43).

Previous studies of uptaking of homologous ssDNA by large negatively supercoiled dsDNA plasmids showed an association rate of 600 $M^{-1}s^{-1}$ at a temperature of 75°C. This reaction led to the removal of superhelical turns in the dsDNA, suggesting that the ssDNA invades into the dsDNA, binds to the complementary strand and forms a D-loop structure (44), which differs from the formation of the parallel triplex observed in this study. In the case of D-loop formation, high temperature decreases the base pair stability of the plasmid dsDNA template and the D-loop structure is further stabilized by negative supercoiling (45,46). In the case of the parallel triplex formation reported in this work, the ssDNA is tethered under a tensile force and the dsDNA is not subject to any negative torsion, which makes the D-loop formation highly energetically unfavorable. In addition, the association of the homologous dsDNA to the stretched ssDNA occurs at room temperature, which also differs from the previous experiments of uptaking of homologous ssDNA to a negatively supercoiled dsDNA plasmid that was facilitated by high temperature. Moreover, the as-

sociation rate of ssDNA to negatively supercoiled dsDNA (600 $M^{-1}s^{-1}$) corresponds to 3×10^{-5} s^{-1} at an ssDNA concentration of 50 nM, which is two orders of magnitude slower than the binding rate of the homologous dsDNA to the stretched ssDNA observed in our experiment ($\sim 3 \times 10^{-3}$ s^{-1} in a dsDNA concentration of 50 nM) (Supplementary Figure S1A), further suggesting different natures of these interactions.

It is also interesting to compare the rate of parallel triplex formation on the mechanically stretched ssDNA with the rate of the initial association of the RecA/Rad51-ssDNA filament with dsDNA, which serves as an early intermediate prior to the base pair switch during HR reaction (47,48). The formation rate of this early intermediate was reported to be in the order of 10^5 $M^{-1}s^{-1}$ corresponding to 5×10^{-3} s^{-1} at a dsDNA substrate concentration of 50 nM (47). This rate is surprisingly similar to the parallel triplex formation rate ($\sim 3 \times 10^{-3}$ s^{-1}) on a stretched ssDNA in the same concentration of dsDNA (Supplementary Figure S1A). It is unclear whether this is a coincidence, so we refrain from further discussion on its potential implications.

The parallel triplex seems to be somewhat related to the triple-stranded joint molecule formed between dsDNA and Mhr1-associated ssDNA. The triple-stranded joint molecule is not in a D-loop structure and remains stable after Mhr1 is removed (43). It was demonstrated that the dsDNA substrate in the joint molecule has the same twist as the B-form duplex (43). All these features are consistent with the parallel triplex formed in our experiments that were conducted in the absence of recombinases. The parallel triplex was also suggested in several experiments after the deproteinization of the RecA-mediated pre-synapse complex (49–53) with stability comparable to the duplex dsDNA (49,50,54). Its presence was unambiguously detected in a recent single-molecule experiment, which traced the dynamics of a dsDNA template during its interaction with an incoming RecA·ATP-ssDNA nucleoprotein filament, throughout several key stages including initial synapse formation, during strand-invasion and after RecA-depolymerization (55). Importantly, after RecA depolymerization, not only the extension of the final product decreased back to the original level of dsDNA, but also the relaxed linking number was indistinguishable from the original B-form dsDNA (55). By using a single-molecule enzyme cleavage assay, the authors showed that the final product is composed of three strands (55). These results strongly suggest the existence of a stable parallel triplex with a regular structure, which has a similar contour length as the B-form duplex, with the displaced ssDNA strand wrapping around the heteroduplex DNA in a right-handed manner with a similar helical pitch of the B-form dsDNA.

In contrast to the reported parallel triplex formed on long DNA catalyzed by RecA, it is very challenging to form such triplex structures by directly incubating ssDNA and homologous dsDNA molecules in the absence of protein. The parallel triplex formed in protein free condition was only reported using specifically designed short oligonucleotides, which behaves less stable compared to the canonical antiparallel triplex (31,56–60). It has been postulated that a high energy barrier may prevent the spontaneous formation of the parallel triplex structures while the conformation change in the DNA strands after initial binding of RecA may lower this energy barrier and thereby allowing the formation of the parallel triplex (53). Our finding that the mechanical stretching of ssDNA can promote the formation of the parallel triplex might provide a clue to the nature of the energy barrier. The extended ssDNA in the RecA-nucleoprotein filament with ssDNA bases that assume a B-form conformation in each triplet unit might be crucial for its interaction with a homologous dsDNA. Interestingly, our Molecular Dynamics (MD) simulations revealed that forces within our experimental range promote a highly ordered right-handed helical conformation of ssDNA in which all bases stack with their neighbors (Supplementary Figure S12). The simulated conformation of ssDNA is similar to the conformation of ssDNA in the triplet unit of the RecA-nucleoprotein filament. On the basis of this similarity, we reason that a local stretch of ssDNA in the base-stacked, right-handed helical conformation, which was produced by force in our experiments or by recombinase, may reduce the energy barrier for parallel triplex formation.

As ssDNA inside the RecA/Rad51-coated nucleoprotein filament is in an extended state, the parallel triplex may form and serve as an important intermediate during RecA/Rad51-catalyzed homologous joint formation. Since all three strands in the RecA/Rad51-catalyzed base-pair-switched homologous joint molecule assume an extended conformation (16), it is possible that the strong homologous ssDNA–dsDNA interaction, in addition to RecA–DNA interaction (22,24), helps to stabilize an extended state of dsDNA during RecA/Rad51-catalyzed homologous joint-molecule formation.

SUPPLEMENTARY DATA

Supplementary Data are available at NAR Online.

ACKNOWLEDGEMENTS

We would like to thank Prof. Maxim Frank-Kamenetskii for proofreading and valuable suggestions.
Author' contributions: J.Y. conceived the research. J.Y. and J.C. designed experiments. J.C., S.G. and C.L. performed the experiments. J.C., S.G. and S.L. performed data analysis. Q.T. performed the simulation. J.C. and J.Y. interpreted the data and wrote the paper.

FUNDING

Singapore Ministry of Education Academic Research Fund Tier 3 [MOE2012-T3-1-001 to J.Y.]; National Research Foundation through the Mechanobiology Institute Singapore [to J.Y.]. Funding for open access charge: Singapore Ministry of Education Academic Research Fund Tier 3 [MOE2012-T3–1-001].
Conflict of interest statement. None declared.

REFERENCES

1. Kowalczykowski,S.C., Dixon,D.A., Eggleston,A.K., Lauder,S.D. and Rehrauer,W.M. (1994) Biochemistry of homologous recombination in Escherichia coli. *Microbiol. Rev.*, **58**, 401–465.

2. Stasiak,A., Di Capua,E. and Koller,T. (1981) Elongation of duplex DNA by recA protein. *J. Mol. Biol.*, **151**, 557–564.
3. Flory,J., Tsang,S.S. and Muniyappa,K. (1984) Isolation and visualization of active presynaptic filaments of recA protein and single-stranded DNA. *Proc. Natl. Acad. Sci. U.S.A.*, **81**, 7026–7030.
4. Nishinaka,T., Ito,Y., Yokoyama,S. and Shibata,T. (1997) An extended DNA structure through deoxyribose-base stacking induced by RecA protein. *Proc. Natl. Acad. Sci. U.S.A.*, **94**, 6623–6628.
5. Chen,Z., Yang,H. and Pavletich,N.P. (2008) Mechanism of homologous recombination from the RecA-ssDNA/dsDNA structures. *Nature*, **453**, 489–484.
6. van Loenhout,M.T., van der Heijden,T., Kanaar,R., Wyman,C. and Dekker,C. (2009) Dynamics of RecA filaments on single-stranded DNA. *Nucleic Acids Res.*, **37**, 4089–4099.
7. Fu,H., Le,S., Chen,H., Muniyappa,K. and Yan,J. (2013) Force and ATP hydrolysis dependent regulation of RecA nucleoprotein filament by single-stranded DNA binding protein. *Nucleic Acids Res.*, **41**, 924–932.
8. Short,J.M., Liu,Y., Chen,S., Soni,N., Madhusudhan,M.S., Shivji,M.K. and Venkitaraman,A.R. (2016) High-resolution structure of the presynaptic RAD51 filament on single-stranded DNA by electron cryo-microscopy. *Nucleic Acids Res.*, **44**, 9017–9030.
9. Xiao,J., Lee,A.M. and Singleton,S.F. (2006) Direct evaluation of a kinetic model for RecA-mediated DNA-strand exchange: the importance of nucleic acid dynamics and entropy during homologous genetic recombination. *Chembiochem*, **7**, 1265–1278.
10. Savir,Y. and Tlusty,T. (2010) RecA-mediated homology search as a nearly optimal signal detection system. *Mol. Cell*, **40**, 388–396.
11. Prentiss,M., Prevost,C. and Danilowicz,C. (2015) Structure/function relationships in RecA protein-mediated homology recognition and strand exchange. *Crit. Rev. Biochem. Mol. Biol.*, **50**, 453–476.
12. Adzuma,K. (1992) Stable synapsis of homologous DNA molecules mediated by the Escherichia coli RecA protein involves local exchange of DNA strands. *Genes Dev.*, **6**, 1679–1694.
13. Gupta,R.C., Folta-Stogniew,E., O'Malley,S., Takahashi,M. and Radding,C.M. (1999) Rapid exchange of A:T base pairs is essential for recognition of DNA homology by human Rad51 recombination protein. *Mol. Cell*, **4**, 705–714.
14. Qi,Z., Redding,S., Lee,J.Y., Gibb,B., Kwon,Y., Niu,H., Gaines,W.A., Sung,P. and Greene,E.C. (2015) DNA sequence alignment by microhomology sampling during homologous recombination. *Cell*, **160**, 856–869.
15. Lee,J.Y., Terakawa,T., Qi,Z., Steinfeld,J.B., Redding,S., Kwon,Y., Gaines,W.A., Zhao,W., Sung,P. and Greene,E.C. (2015) DNA RECOMBINATION. Base triplet stepping by the Rad51/RecA family of recombinases. *Science*, **349**, 977–981.
16. Xiao,J. and Singleton,S.F. (2002) Elucidating a key intermediate in homologous DNA strand exchange: structural characterization of the RecA-triple-stranded DNA complex using fluorescence resonance energy transfer. *J. Mol. Biol.*, **320**, 529–558.
17. Smith,S.B., Cui,Y. and Bustamante,C. (1996) Overstretching B-DNA: the elastic response of individual double-stranded and single-stranded DNA molecules. *Science*, **271**, 795–799.
18. Cluzel,P., Lebrun,A., Heller,C., Lavery,R., Viovy,J.L., Chatenay,D. and Caron,F. (1996) DNA: an extensible molecule. *Science*, **271**, 792–794.
19. Zhang,X., Chen,H., Fu,H., Doyle,P.S. and Yan,J. (2012) Two distinct overstretched DNA structures revealed by single-molecule thermodynamics measurements. *Proc. Natl. Acad. Sci. U.S.A.*, **109**, 8103–8108.
20. Zhang,X., Chen,H., Le,S., Rouzina,I., Doyle,P.S. and Yan,J. (2013) Revealing the competition between peeled ssDNA, melting bubbles, and S-DNA during DNA overstretching by single-molecule calorimetry. *Proc. Natl. Acad. Sci. U.S.A.*, **110**, 3865–3870.
21. Kurumizaka,H., Aihara,H., Ikawa,S., Kashima,T., Bazemore,L.R., Kawasaki,K., Sarai,A., Radding,C.M. and Shibata,T. (1996) A possible role of the C-terminal domain of the RecA protein. A gateway model for double-stranded DNA binding. *J. Biol. Chem.*, **271**, 33515–33524.
22. Leger,J.F., Robert,J., Bourdieu,L., Chatenay,D. and Marko,J.F. (1998) RecA binding to a single double-stranded DNA molecule: a possible role of DNA conformational fluctuations. *Proc. Natl. Acad. Sci. U.S.A.*, **95**, 12295–12299.
23. Kurumizaka,H., Ikawa,S., Sarai,A. and Shibata,T. (1999) The mutant RecA proteins, RecAR243Q and RecAK245N, exhibit defective DNA binding in homologous pairing. *Arch. Biochem. Biophys.*, **365**, 83–91.
24. Fu,H., Le,S., Muniyappa,K. and Yan,J. (2013) Dynamics and regulation of RecA polymerization and de-polymerization on double-stranded DNA. *PLoS One*, **8**, e66712.
25. Chen,H., Fu,H., Zhu,X., Cong,P., Nakamura,F. and Yan,J. (2011) Improved high-force magnetic tweezers for stretching and refolding of proteins and short DNA. *Biophys. J.*, **100**, 517–523.
26. Frank-Kamenetskii,M.D. and Mirkin,S.M. (1995) Triplex DNA structures. *Annu. Rev. Biochem.*, **64**, 65–95.
27. Le,S., Yao,M., Chen,J., Efremov,A.K., Azimi,S. and Yan,J. (2015) Disturbance-free rapid solution exchange for magnetic tweezers single-molecule studies. *Nucleic Acids Res.*, **43**, e113.
28. Le,S., Chen,H., Zhang,X., Chen,J., Patil,K.N., Muniyappa,K. and Yan,J. (2014) Mechanical force antagonizes the inhibitory effects of RecX on RecA filament formation in Mycobacterium tuberculosis. *Nucleic Acids Res.*, **42**, 11992–11999.
29. You,H., Zeng,X., Xu,Y., Lim,C.J., Efremov,A.K., Phan,A.T. and Yan,J. (2014) Dynamics and stability of polymorphic human telomeric G-quadruplex under tension. *Nucleic Acids Res.*, **42**, 8789–8795.
30. Brosey,C.A., Chagot,M.E., Ehrhardt,M., Pretto,D.I., Weiner,B.E. and Chazin,W.J. (2009) NMR analysis of the architecture and functional remodeling of a modular multidomain protein, RPA. *J. Am. Chem. Soc.*, **131**, 6346–6347.
31. Vlieghe,D., Van Meervelt,L., Dautant,A., Gallois,B., Precigoux,G. and Kennard,O. (1996) Parallel and antiparallel (G.GC)2 triple helix fragments in a crystal structure. *Science*, **273**, 1702–1705.
32. Chen,J., Le,S., Basu,A., Chazin,W.J. and Yan,J. (2015) Mechanochemical regulations of RPA's binding to ssDNA. *Sci. Rep.*, **5**, 9296.
33. Gore,J., Bryant,Z., Nollmann,M., Le,M.U., Cozzarelli,N.R. and Bustamante,C. (2006) DNA overwinds when stretched. *Nature*, **442**, 836–839.
34. Fu,H., Chen,H., Marko,J.F. and Yan,J. (2010) Two distinct overstretched DNA states. *Nucleic Acids Res.*, **38**, 5594–5600.
35. King,G.A., Gross,P., Bockelmann,U., Modesti,M., Wuite,G.J. and Peterman,E.J. (2013) Revealing the competition between peeled ssDNA, melting bubbles, and S-DNA during DNA overstretching using fluorescence microscopy. *Proc. Natl. Acad. Sci. U.S.A.*, **110**, 3859–3864.
36. Zhang,X., Qu,Y., Chen,H., Rouzina,I., Zhang,S., Doyle,P.S. and Yan,J. (2014) Interconversion between three overstretched DNA structures. *J. Am. Chem. Soc.*, **136**, 16073–16080.
37. Fu,H., Chen,H., Zhang,X., Qu,Y., Marko,J.F. and Yan,J. (2011) Transition dynamics and selection of the distinct S-DNA and strand unpeeling modes of double helix overstretching. *Nucleic Acids Res.*, **39**, 3473–3481.
38. Kochoyan,M., Leroy,J.L. and Gueron,M. (1987) Proton exchange and base-pair lifetimes in a deoxy-duplex containing a purine-pyrimidine step and in the duplex of inverse sequence. *J. Mol. Biol.*, **196**, 599–609.
39. Shibata,T., Nishinaka,T., Mikawa,T., Aihara,H., Kurumizaka,H., Yokoyama,S. and Ito,Y. (2001) Homologous genetic recombination as an intrinsic dynamic property of a DNA structure induced by RecA/Rad51-family proteins: a possible advantage of DNA over RNA as genomic material. *Proc. Natl. Acad. Sci. U.S.A.*, **98**, 8425–8432.
40. Li,Z., Karakousis,G., Chiu,S.K., Reddy,G. and Radding,C.M. (1998) The beta protein of phage lambda promotes strand exchange. *J. Mol. Biol.*, **276**, 733–744.
41. Kumar,J.K. and Gupta,R.C. (2004) Strand exchange activity of human recombination protein Rad52. *Proc. Natl. Acad. Sci. U.S.A.*, **101**, 9562–9567.
42. Bi,B., Rybalchenko,N., Golub,E.I. and Radding,C.M. (2004) Human and yeast Rad52 proteins promote DNA strand exchange. *Proc. Natl. Acad. Sci. U.S.A.*, **101**, 9568–9572.
43. Ling,F., Yoshida,M. and Shibata,T. (2009) Heteroduplex joint formation free of net topological change by Mhr1, a mitochondrial recombinase. *J. Biol. Chem.*, **284**, 9341–9353.
44. Wiegand,R.C., Beattie,K.L., Holloman,W.K. and Radding,C.M. (1977) Uptake of homologous single-stranded fragments by

superhelical DNA. III. The product and its enzymic conversion to a recombinant molecule. *J. Mol. Biol.*, **116**, 805–824.
45. Holloman,W.K., Wiegand,R., Hoessli,C. and Radding,C.M. (1975) Uptake of homologous single-stranded fragments by superhelical DNA: a possible mechanism for initiation of genetic recombination. *Proc. Natl. Acad. Sci. U.S.A.*, **72**, 2394–2398.
46. Beattie,K.L., Wiegand,R.C. and Radding,C.M. (1977) Uptake of homologous single-stranded fragments by superhelical DNA. II. Characterization of the reaction. *J. Mol. Biol.*, **116**, 783–803.
47. Gupta,R.C., Folta-Stogniew,E. and Radding,C.M. (1999) Human Rad51 protein can form homologous joints in the absence of net strand exchange. *J. Biol. Chem.*, **274**, 1248–1256.
48. Folta-Stogniew,E., O'Malley,S., Gupta,R., Anderson,K.S. and Radding,C.M. (2004) Exchange of DNA base pairs that coincides with recognition of homology promoted by E. coli RecA protein. *Mol. Cell*, **15**, 965–975.
49. Hsieh,P., Camerini-Otero,C.S. and Camerini-Otero,R.D. (1990) Pairing of homologous DNA sequences by proteins: evidence for three-stranded DNA. *Genes Dev.*, **4**, 1951–1963.
50. Rao,B.J., Dutreix,M. and Radding,C.M. (1991) Stable three-stranded DNA made by RecA protein. *Proc. Natl. Acad. Sci. U.S.A.*, **88**, 2984–2988.
51. Rao,B.J., Chiu,S.K. and Radding,C.M. (1993) Homologous recognition and triplex formation promoted by RecA protein between duplex oligonucleotides and single-stranded DNA. *J. Mol. Biol.*, **229**, 328–343.
52. Camerini-Otero,R.D. and Hsieh,P. (1993) Parallel DNA triplexes, homologous recombination, and other homology-dependent DNA interactions. *Cell*, **73**, 217–223.
53. Cox,M.M. (1995) Alignment of 3 (but not 4) DNA strands within a RecA protein filament. *J. Biol. Chem.*, **270**, 26021–26024.
54. Rao,B.J., Jwang,B. and Radding,C.M. (1990) RecA protein reinitiates strand exchange on isolated protein-free DNA intermediates. An ADP-resistant process. *J. Mol. Biol.*, **213**, 789–809.
55. van der Heijden,T., Modesti,M., Hage,S., Kanaar,R., Wyman,C. and Dekker,C. (2008) Homologous recombination in real time: DNA strand exchange by RecA. *Mol. Cell*, **30**, 530–538.
56. Shchyolkina,A.K., Timofeev,E.N., Borisova,O.F., Il'icheva,I.A., Minyat,E.E., Khomyakova,E.B. and Florentiev,V.L. (1994) The R-form of DNA does exist. *FEBS Lett.*, **339**, 113–118.
57. Dagneaux,C., Liquier,J. and Taillandier,E. (1995) FTIR study of a nonclassical dT10*dA10-dT10 intramolecular triple helix. *Biochemistry*, **34**, 14815–14818.
58. Spink,N., Nunn,C.M., Vojtechovsky,J., Berman,H.M. and Neidle,S. (1995) Crystal structure of a DNA decamer showing a novel pseudo four-way helix-helix junction. *Proc. Natl. Acad. Sci. U.S.A.*, **92**, 10767–10771.
59. Dagneaux,C., Gousset,H., Shchyolkina,A.K., Ouali,M., Letellier,R., Liquier,J., Florentiev,V.L. and Taillandier,E. (1996) Parallel and antiparallel A*A-T intramolecular triple helices. *Nucleic Acids Res.*, **24**, 4506–4512.
60. Shchyolkina,A.K., Borisova,O.F., Minyat,E.E., Timofeev,E.N., Il'icheva,I.A., Khomyakova,E.B. and Florentiev,V.L. (1995) Parallel purine-pyrimidine-purine triplex: experimental evidence for existence. *FEBS Lett.*, **367**, 81–84.